Viscous Effects on Biowaste Resistojet Nozzle Performance

JAMES M. KALLIS* AND MILTON GOODMAN†
McDonnell Douglas Corporation, Huntington Beach, Calif.
AND
CARL R. HALBACH‡
Advanced Rocket Technology (ARTCOR), Irvine, Calif.

Viscous effects on the performance of biowaste resistojet microthrusters are calculated using Rae's numerica method for low-Reynolds number flow in a nozzle. Results are presented for a 25-mlb thruster suitable for space station attitude control using CO_2, CH_4, and H_2O as propellants. Nozzle exit plane data (such as Mach number, velocity, and temperature profiles) useful for computations of plume contamination are also presented. The performance predictions are compared with experimental data which were available from laboratory firings of a 10-mlb thruster having a trumpet-shaped nozzle with CO_2, CH_4, H_2O and H_2 as propellants.

Nomenclature

B = Reynolds number [see Eq. (2)]
C_D = nozzle discharge coefficient
C_F = thrust coefficient
CMG = control moment gyro
D^* = nozzle throat diameter
F = thrust
H = specific enthalpy
I_{sp} = specific impulse
M_ℓ = centerline Mach number
MW = molecular weight
$\dot{m}$ = mass flow rate
P = power
Pr = Prandtl number
p = pressure
R = universal gas constant
r = radial coordinate, measured from nozzle axis
r^*, r_w = nozzle throat, local nozzle radius
T = temperature
u = velocity
x = z/r^*
z = axial coordinate, measured from nozzle throat
γ = specific-heat ratio
ΔV = velocity increment
δ_1 = boundary-layer displacement thickness
ϵ = nozzle area ratio
η = r/r_w or over all total power efficiency
θ_1 = nozzle inlet convergence half angle (see Fig. 4)
μ = viscosity
ρ = density
ω = exponent in the relation $\mu \alpha T^\omega$

Subscript

$(\ )_0$ = conditions in chamber, i.e., downstream end of heater

Presented as Paper 72-450 at the AIAA 9th Electric Propulsion Conference, Bethesda, Md., April 17–19, 1972; submitted April 17, 1972; revision received August 2, 1972. This research was partially supported by the McDonnell Douglas Astronautics Company's Independent Research and Development Program. The authors wish to thank the following individuals for their valuable suggestions and contributions in developing the data for this paper: W. J. Rae, Cornell Aeronautical Laboratory; R. J. Page, Advanced Rocket Technology (ARTCOR); R. V. Greco, McDonnell Douglas Astronautics Company.

Index categories: Spacecraft Propulsion Systems Integration; Electric and Advanced Space Propulsion; Nozzle and Channel Flow.

* Senior Engineer/Scientist, Propulsion Department, Research and Development. Member AIAA.

† Senior Technical Specialist, MDAC-East. Associate Fellow AIAA.

‡ Director of Engineering. Member AIAA.

Introduction

MANNED space station studies[1] have resulted in the selection of low-thrust attitude control resistojets which use the excess biowaste by-products (CH_4, CO_2, and H_2O) from the life support oxygen recovery cycle as propellant. This use of the biowaste by-products reduces the over-all system weight by eliminating or greatly reducing the resupply requirements while providing an efficient method for biowaste disposal.

Each of the propellants has an upper temperature limit to which it can be heated to minimize undesirable side reactions. Thus, a single universal thruster design must satisfy the vehicle requirements for thrust, torque, and impulse per orbit while operating at minimum power and propellant consumption. It is, therefore, important to predict accurately the propulsion performance for the varying conditions of thruster operation.

Computer programs using both equilibrium and non-equilibrium chemistry have been applied to the heater portion for determining propellant characteristics and ideal heater electric power requirements, while one-dimensional isentropic flow programs have been used to determine the desired propulsion parameters (specific impulse, thrust coefficient, etc.) as well as possible exhaust plume contamination effects.[2] However, because of their small size, the microthrusters may have relatively thick boundary layers and large viscous losses in the nozzle. As a result, the performance and nozzle exit flowfield can be significantly different than for inviscid flow computations.

In this study, viscous effects on nozzle performance have been computed for the first time for the biowaste propellants, using the Rae slender nozzle program.[3] In addition, the analytical results for a trumpet nozzle have been compared with published test results[4] and have shown good agreement.

Biowaste Resistojet System

The stabilization system for manned space stations consists of control moment gyros augmented by reaction control thrusters which develop torques about the three axes to provide gimbal desaturation and to perform station keeping functions. Past studies[1] have demonstrated that a substantial saving in over-all system weight is achieved by using the expendable biowaste by-products resulting from the life support oxygen recovery cycle for propellant in a resistojet reaction control system. This eliminates the need for propellant resupply and decreases the external contamination problem, which could result from haphazard dumping to space.

A candidate oxygen recovery system is the Sabatier methane process. H_2 is reacted with the CO_2 separated from the cabin

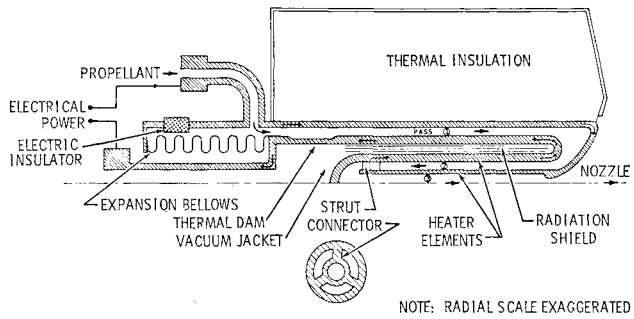

Fig. 1 Biowaste resistojet.

air, the reaction products being CH_4 and H_2O. Electrolysis of the H_2O produces O_2, which is recycled back to the cabin air makeup while the H_2 is returned to the Sabatier reactor. The CH_4 and the excess CO_2 and water (approximately 15 lb/day from a 9-man crew) are collected, stored separately, and fed on demand to the thruster system.

The latter consists of 16 or more 25-mlb thrust level resistojets mounted in 4 modules about the space station periphery. The thrusters operate singly or in pairs to generate the required torques or translational thrust. The successful operation of the system involves the matching of vehicle requirements for thrust level and desired impulse per orbit with the availability of propellant mass, type, and electric power for a given optimized thruster design.

A typical thruster considered for space station applications is shown in Fig. 1. This resistojet, of the evaculated concentric tubular type, has been described in previous papers.[1,5,6] Ohmic heating takes place in the series-connected heating elements, and the propellant, entering at the outer annulus, makes three traversals before achieving its maximum chamber temperature at the nozzle throat entrance. Thereafter, the gas is expanded through the nozzle to develop its thrust.

The following formula relates the thrust, electric power input, and developed specific impulse:

$$F = 45.9\eta P/I_{sp} \tag{1}$$

where F = thrust, lb ; P = power to terminal, kw; I_{sp} = specific impulse, sec; η = over-all total power efficiency = jet power/(electric power + inlet propellant power).

The over-all total power efficiency η is a complicated function of thruster design (heater efficiency, thermal radiation losses, nozzle efficiency) and of propellant reaction kinetics. As a result, η has heretofore been best determined by actual physical testing.

The propulsion system designer is faced with the immediate problem of predicting the thruster performance using the three propellants CH_4, CO_2, and H_2O singly or in mixtures in a single thruster geometry while satisfying a broad range of control system demands for CMG gimbal desaturation, translational ΔVs, and station keeping under varying conditions of gas flow rate, chamber temperature, and pressure. It has therefore been necessary to augment the limited physical testing with analytical techniques to predict system performance. The heater portion of the resistojet has been analyzed with computer programs which use both equilibrium chemistry and chemical kinetics to predict propellant properties, and also the minimum theoretical power needed to achieve a specified chamber temperature consistent with each type of propellant.

The I_{sp} has been computed for successive nozzle area or pressure ratios using equilibrium or frozen chemistry with isentropic one-dimensional flow. This inviscid I_{sp} has then been modified using experimental correlations in order to predict real performance parameters since heretofore no nozzle program has been available with which to directly compute the thruster performance for low-Reynolds-number flow. Such a program has recently become available and has been used to analyze the nozzle performance with the biowaste propellants, as described in the following section.

Method of Calculation

The performance prediction method uses an improved version of a numerical solution developed by Rae[3] for viscous flow in a nozzle. This method is based on the slender-channel approximation to the Navier-Stokes equations. The slender-channel equations, which are derived by assuming that the nozzle walls converge and diverge slowly, are formally identical with the boundary layer equations. In this approximation, the pressure varies only with axial position in the nozzle, while the other quantities (velocity, temperature, etc.) vary with both radial and axial position. The equations are written in cylindrical coordinates aligned with the nozzle axis. The boundary conditions are applied on the axis and at the wall. On the axis, the radial derivatives of all variables vanish as a result of axial symmetry. At the wall, rarefied-flow boundary conditions, which allow a velocity slip and a temperature jump, are used.

Starting at a station far upstream of the nozzle throat, the slender-channel equations are solved in successive downstream steps by an implicit finite-difference scheme. Rae's method applies the slender-channel equations across the nozzle cross section, thus precluding the need to assume that the viscous region is confined to a thin boundary layer adjacent to the nozzle wall. The method is, therefore, advantageous for the analysis of the resistojet nozzles, where the Reynolds number is so low that the viscous region extends almost or entirely across the nozzle cross section.

In contrast with nozzle performance calculations that use the thin-boundary-layer approximation, the nozzle discharge coefficient is not known a priori in Rae's method and hence must be found by iteration. Given an estimate of the discharge coefficient, the flow is calculated from the starting station downstream through the throat. The estimated discharge coefficient is too low if the pressure gradient dp/dx becomes positive, and is too high if the pressure gradient remains negative but becomes larger in magnitude than a specified value. After the discharge coefficient is compute to a predetermined accuracy, a final computation is made, starting upstream of the throat and proceeding downstream to the exit plane.

The main input parameter is a Reynolds number based on reservoir conditions and the throat radius

$$B \equiv \rho_0(2H_0)^{1/2}r^*/\mu_0 = [2\gamma/(\gamma-1)]^{1/2}(MW/RT_0)^{1/2}\, p_0 r^*/\mu_0 \tag{2}$$

where the characteristic velocity is the maximum adiabatic velocity $(2H_0)^{1/2}$. The value of B is typically several times larger than the Reynolds number based on the throat conditions and the throat radius.

Rae's method assumes that the gas is thermally and calorically perfect and that its chemical composition is frozen at the chamber composition. For the cases calculated in the present study, the adiabatic-wall boundary conditions were used. The adiabatic wall is a good approximation for the buried, radiation-shielded nozzle under consideration here (see Fig. 1). Furthermore, it was assumed that the gas undergoes no reaction as it passes through the heater.

In the present study, several improvements were made in Rae's computational scheme. Some of these improvements were made in the details of the iterative procedure and have speeded up the calculation without loss of accuracy. (A typical case requires about 15 min of computation time on a CDC 6500 computer. The time depends mostly on the accuracy of the initial estimates of the discharge coefficient and on the length of the nozzle compared with the throat radius.)

Table 1 Physical properties of propellants

Gas	γ	Pr	ω
CH_4	1.14	1.08	1.00
CO_2	1.17	0.96	1.00
H_2O	1.21	0.77	1.00
H_2[a]	1.40	0.78	0.64

[a] Only trace amounts of H_2 would normally be present in the Sabatier expendables.

The other improvement extended the range of operation of Rae's method. As received, Rae's computer program could be used only for a nozzle contour consisting of a convergent cone and a divergent cone, connected by a constant-radius-of-curvature section. In the present study the nozzle geometry coding, which is conveniently contained in a single subroutine, was generalized to allow the contour to be specified by tabular coordinates. The tabular option was used for the trumpet nozzle discussed below. It was also found that Rae's method could be used successfully beyond the range for which the slender-channel approximation would be expected to be accurate. Whereas Rae had never used his method for values of B higher than 3000 or for conical inlet angles steeper than $\theta_1 = -30°$, successful runs have been made in the present study for values of B as high as 13,000 and for $\theta_1 = -45°$.

Results for 25-mlb Thruster

The computation method has been applied to a 25-mlb thruster suitable for space station attitude control. The chamber pressure was $p_0 = 3$ atm, and each of the propellants CH_4, CO_2, and H_2O was studied separately. Mixtures of the gases, however, can be treated similarly. These conditions were also used in the performance calculations reported in Ref. 2. The present calculations were made for a conical nozzle with an 18° divergence half angle, an expansion ratio of 100, and a throat radius of 0.0098 in. As in Ref. 2, a chamber temperature $T_0 = 2880°$R was used for CO_2 and H_2O, and 1800°R was used for CH_4 since it tends to decompose and form a carbon deposition above 1800°R. The physical properties of the propellants are given in Table 1. The quantity ω is the exponent in the relation $\mu \propto T^{\omega}$, which is used in Rae's method to describe the dependence of viscosity on temperature. The values in Table 1 are intended as average values for the nozzle expansion. The values of B are 8980 for CH_4, 8220 for CO_2, and 5170 for H_2O.

In Fig 2, the calculated vacuum specific impulse is plotted against nozzle area ratio for each of the three propellants. Also plotted in the vacuum specific impulse for an isentropic one-dimensional expansion to the area ratio ε. The corresponding thrust coefficient is given by

$$C_{F_{\text{inviscid}}} = \left[\frac{2\gamma^2}{\gamma-1}\left(\frac{2}{\gamma+1}\right)^{(\gamma+1)/(\gamma-1)}\left(1-\frac{p}{p_0}\right)^{(\gamma-1)/\gamma}\right]^{1/2} + \frac{p}{p_0}\varepsilon \qquad (3)$$

where p/p_0 is the pressure ratio corresponding to an isentropic expansion for the area ratio ε. The specific impulse is related to the thrust coefficient by

$$I_{sp} = \frac{\gamma-1}{4\gamma}\left(\frac{\gamma+1}{2}\right)^{1/(\gamma-1)}\left(\frac{\gamma+1}{\gamma-1}\right)^{1/2}\frac{2}{C_D}(2H_0)^{1/2}C_F \qquad (4)$$

Since γ, C_D, and H_0 are independent of ε, the quantities I_{sp} and C_F vary with ε in the same way. Henceforth, we shall use I_{sp} and C_F interchangeably as measures of the nozzle performance. Viscous effects are seen to lower I_{sp} about 10% below the inviscid value. Since the computed specific impulse rapidly approaches an asymptotic value with increasing ε, a nozzle cut off at a much smaller area ratio than 100 would provide almost the same thrust as the $\varepsilon = 100$ nozzle. This result was also noted by Rae.

Although the thruster performance is the most important quantity obtained from the computation method, useful information on details of the flowfield is also obtained. Some of these flowfield data are plotted in Figs. 3–7. The velocity

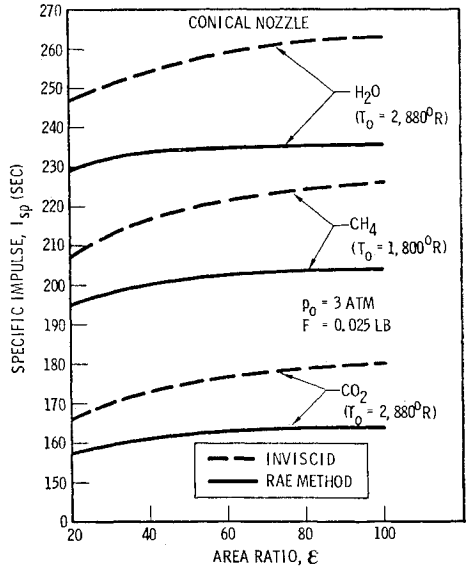

Fig. 2 Performance of 25-mlb thruster.

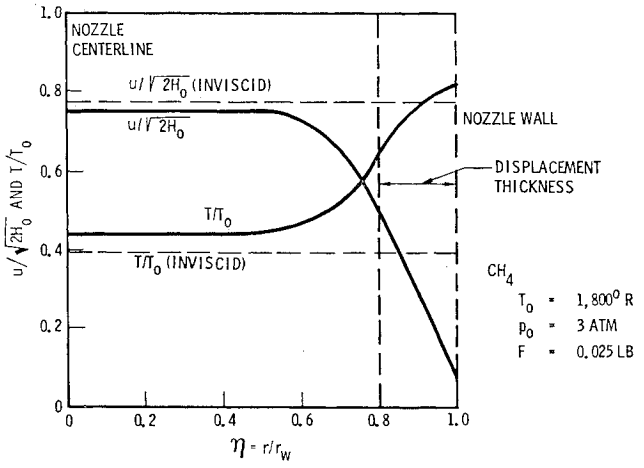

Fig. 3a Nozzle exit plane flowfield, CH_4.

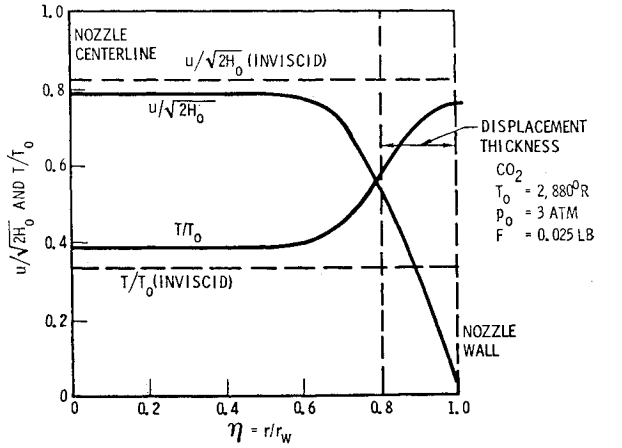

Fig. 3b Nozzle exit plane flowfield, CO_2.

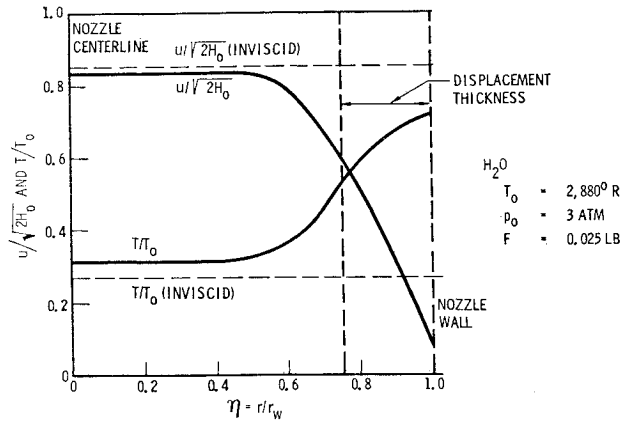

Fig. 3c Nozzle exit plane flowfield, H_2O.

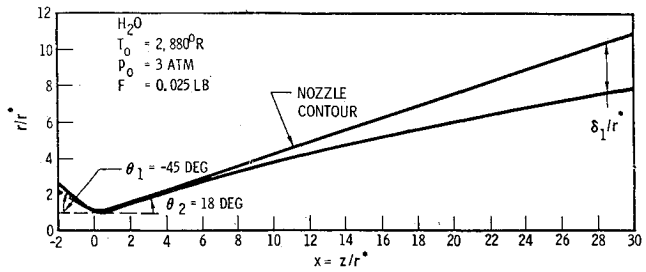

Fig. 4 Boundary-layer displacement thickness.

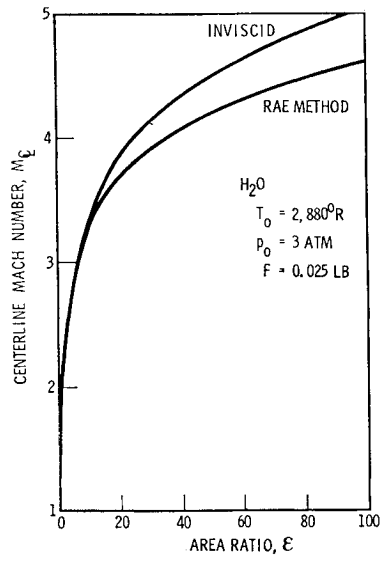

Fig. 5 Centerline Mach number vs area ratio.

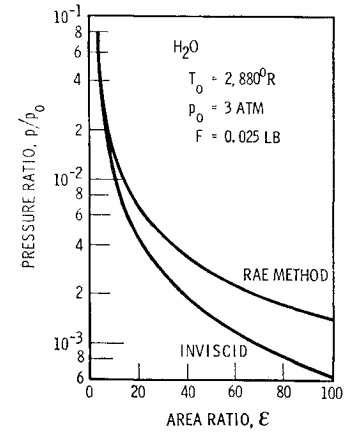

Fig. 6 Pressure vs area ratio.

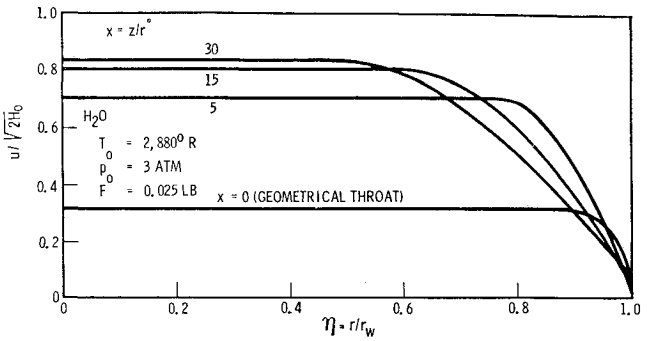

Fig. 7 Development of velocity profile.

and temperature profiles at the nozzle exit plane for each of the propellants are shown in Fig. 3. The boundary-layer displacement thickness is about 19% of the nozzle exit radius for CH_4 and CO_2, and is about 25% for H_2O. For each of the propellants, however, significant departures from uniformity in these profiles begin about halfway between the axis and the wall ($\eta = 0.5$). The exit-plane data can be used as inputs to a plume flowfield calculation for prediction of spacecraft plume contamination, among other applications.

Figures 4–7 show the flowfield inside the nozzle. The results are shown only for the H_2O case which, having the lowest Reynolds number, has the most pronounced viscous effects. The results for CH_4 and CO_2 are similar. Figure 4 shows the boundary-layer growth as the gas flows downstream. Figures 5 and 6 show the deviation of the centerline Mach number and the pressure from the inviscid (isentropic flow) values as the gas flows downstream. Figure 7 shows the development of the velocity profile as downstream distance increases. These data provide insight into the development of the viscous effects and show the effects of cutting off the nozzle at a smaller area ratio.

Some of the flowfield details predicted by Rae's method have been verified experimentally.[3,7] In the next section, the over-all performance predictions are compared with experiments.

Comparison with 10-mlb Thruster Experiments

Description of Experiments

Reference 4 presents data obtained from 10-mlb biowaste resistojet tests used here for comparison with calculated performance. No data were available on 25-mlb size biowaste resistojets. Propellants used in the tests included H_2, H_2O, CH_4, and CO_2, and mixtures of CO_2/CH_4, CO_2/H_2O, and H_2O/CH_4. Thrust was measured to within 0.2% using a balanced single-vertical axis beam.

As part of each thruster-propellant test, the thrust beam was calibrated for cell circulation effects with a thruster nozzle simulator mounted adjacent to the beam but not attached to it. Circulation around the thrust beam/thruster setup was duplicated and its effect on indicated thrust documented. Circulation corrections were then applied to the measured thruster performance. In general, the cell circulation resulted in a thrust defect by torquing the beam opposite to the thruster produced torque. The thrust defect was of the order of 0.2-mlb and varied with cell pressure passing through a maximum at about 1 μ of mercury. The thrust defect varied also with type of propellant and mass flow rate and correlated rather well with the ratio of propellant mass flow rate to the square root of the propellant molecular weight.

For the 10-mlb thruster, another thrust defect was shown[4] to occur for cell pressures above about $\frac{1}{2}\mu$. This is believed to be due to cell pressure feeding back upstream in the divergent nozzle via the thick subsonic portion of the boundary

layer. The effects of varying cell pressures were documented establishing this thrust defect trend. Minor corrections to a hard vacuum condition have been included[4] in the experimental data used here. In all cases, actual test conditions were at less than two microns and the cell pressure corrections made were no more than 1.0% of thrust.

For the 10-mlb thruster data compared here, measured specific impulse errors are considered to be not more than 1.0%. Of all of the propellants used, hydrogen mass flow rate was measured with the least error by using highly sensitive scales. Flow-metering repeatability was better than 0.2%. This high degree of resolution permitted a relatively accurate determination of thrust changes due, for example, to carbon deposition when methane propellant was heated to too high a temperature or to small changes in the cell pressure.

Neither chamber pressure nor temperature was measured directly in the 10-mlb biowaste resistojet. To do so would have been difficult and would have greatly compromised the thruster structurally. Instead, the propellant supply pressure and various structural temperatures were measured accurately during the tests. The chamber pressure was deduced from pressure-drop calculations for the flow passages between the supply pressure fitting and the thruster nozzle. Cold flow chamber pressure was accurately found from a mass continuity calculation. For hot flow conditions, the chamber pressure from a mass continuity calculation required a chamber temperature input.

Chamber temperature, that is the effective total temperature of the propellant entering the thruster exhaust nozzle, was determined from an energy balance calculation and checked by relating inner structure temperature measurements to a heat-transfer model solution. The energy balance method is more accurate than the heat-transfer method.

During the tests the thruster was instrumented externally with sufficient thermocouples to permit detailed calculations of radiation heat transfer between the thruster outer case and the surrounding cold test facility walls. Convective losses at the cell pressures tested (2 μ and less) were negligible. Thermal losses across the insulated thruster mounting bracket and electrical leads were also accounted for.

The power in the gas is the sum of the input electric power and the power brought in with the entering gas less the heat losses [Eq. (5)]. The corresponding gas enthalpy is given by Eq. (6).

$$P_{\text{gas}} = P_{\text{elec}} + P_{\text{prop}} - P_{\text{loss}} \tag{5}$$

$$H_{\text{gas final}} = H_{\text{gas initial}} + P_{\text{gas}}/\dot{m} \tag{6}$$

The gas temperature corresponding to the enthalpy is obtained from a Mollier table or chart, and is believed to be accurate to within $\pm 3\%$.

During thruster tests, a pyrometer sighting was made along the center line through the expansion bellows assembly (see Fig. 1) into the vacuum jacket to the closed heater end forming the transition from gas passage 2 to 3. In addition, thermocouples were located along the outer wall of gas passage 1. An electrical resistance reading was taken over the innermost heater element, seen in Fig. 1 to divide gas passage 2 from 3. This resistance measurement was used to evaluate the mean wall temperature of the innermost heater element from resistivity data. From these structural temperatures, the chamber temperature was calculated from analytical heat-transfer solutions as a back-up or rough check on the energy balance method.

The experimental data used for comparison with the predictions are presented in Table 2. Included are nozzle throat Reynolds numbers based on diameter and on viscosity taken at chamber conditions.

$$Re_{D^*} = 4\dot{m}/\pi D^* \mu_0 \tag{7}$$

This Reynolds number, different from B used by Rae, is shown in the table for convenience as it is generally used to correlate flow-discharge coefficients. Thruster nozzle discharge coefficients for the experimental data points considered are also listed.

Trumpet Nozzle

A trumpet-shaped nozzle was used in these experiments to provide improved performance as well as increase structural rigidity between the inner heater element and the outer case.[4,6] For a highly viscous nozzle flow ($Re_{D^*} < 4000$), it can be shown analytically that a slightly trumpet-shaped nozzle is more efficient than a conical nozzle. Relative to a conical nozzle, expansion efficiency can be improved more than divergence efficiency decreases by using the trumpet shaping.

The nozzle contour is plotted in Fig. 8. The throat radius is 0.009 in. The pass-3 heater tube (see Fig. 1) from which the propellant enters the nozzle has a radius of 0.020 in; therefore, the area ratio upstream of the throat is 5. The throat section has a constant radius of curvature of 0.010 in., and the radius of curvature is constant downstream of the throat out to where the nozzle divergence half angle is 12.2° and the area ratio is 1.1. Downstream of the $\varepsilon = 147$ point, the nozzle is conical with a divergence half angle of 35°. The over-all nozzle expansion ratio is 360.

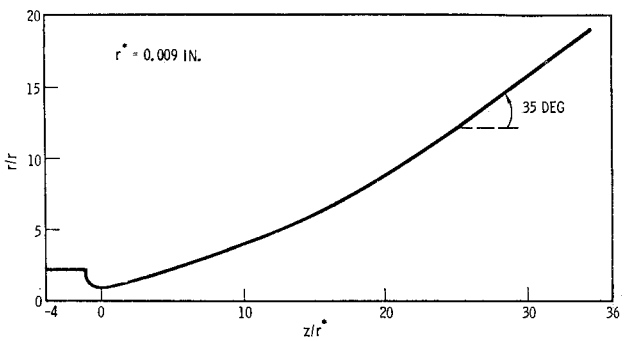

Fig. 8 Trumpet nozzle.

Table 2 Biowaste resistojet experimental data

Propellant	Measured directly			Deduced				
	F mlb	I_{sp} sec	P_{supply} atm	T_0 °R	p_0 atm	γ_0	R_{eD^*}	C_D
H_2	12.7	436	2.52	1400	2.3	1.39	2170	0.92
H_2	11.5	630	2.52	3000	2.2	1.33	820	0.89
H_2O	13.8	161	2.52	1260	2.1	1.29	4410	0.95
H_2O	12.2	235	2.52	2800	2.0	1.21	1220	0.90
CO_2	13.5	143	2.52	2200	2.1	1.17	2330	0.93
CH_4	11.5	172	2.04	1200	1.8	1.17	4050	0.94
CH_4	11.0	227	2.04	1800	1.7	1.12[a]	2100	0.92

[a] The value of $\gamma_0 = 1.12$ corresponds to unreacted methane. Equilibrium (reacted) conditions would result in a higher value of $\gamma_0 = 1.27$ Reaction kinetics are considered to favor the unreacted case.

The actual nozzle inlet geometry could not be used in the performance calculations because Rae's computer program cannot handle sharply converging or diverging channels. In the performance prediction runs made for the trumpet nozzle, the inlet was taken to be a cone with a 45° convergence half angle, with a smooth transition into the constant-radius-of-curvature throat section. The conical inlet extends upstream of the throat to an area ratio of 6. Rae's results indicate that the upstream geometry has little effect on the flow downstream of the throat.[3] In the performance-prediction runs, moreover, the computed flowfield changed very little from that at the starting station until just upstream of the throat, where the area ratio was about 2. Hence, the use of this fictitious inlet was expected to have a negligible effect on the predicted performance.

Results and Discussion

The predicted and measured performance values were compared for the following seven cases: CH_4, H_2O, and H_2 at the highest chamber temperature tested and at a lower temperature, and CO_2 at the highest temperature tested. The flowfield details for these seven cases are qualitatively similar to those for the 25-mlb thruster plotted in Figs. 2–7. The low-temperature CO_2 case was not run on Rae's computer program because the Reynolds number is so high that the computation method could not be applied. The computer run for the low-temperature CO_2 case terminated upstream of the nozzle throat because the iteration schemes could not converge at such a high Reynolds number. The Rae method becomes identical with the thin-boundary-layer approximation at high Reynolds numbers. Hence the I_{sp} for low-temperature CO_2 could be, but was not in the present work, calculated by a standard boundary-layer method. The chamber pressure used in the performance predictions is 2.0 atm for the CH_4 cases and 2.4 atm for the other cases. The difference between these rounded values and those of Table 2 have a negligible effect on the predicted performance. The physical properties listed in Table 2 were used in the computer runs. The low-temperature H_2O run corresponds to the minimum heater power used for this propellant. Since the saturation temperature for steam at 2.4 atm is 720°R, the engine was operating with 540°R of superheat in the minimum-power H_2O runs.

Comparison of predicted and measured thruster performance is shown in Table 3. The cases are listed in increasing order of the Reynolds number B. For each propellant and chamber temperature, the table shows the predicted and measured values of specific impulse along with the percent difference relative to the measured value. The remaining table entries are discussed later.

The agreement between the predicted and measured values of I_{sp} is seen to be quite close, verifying the accuracy of the performance-prediction method. The closest agreement is with the H_2 data, the most accurate of the experimental data. Possible explanations for the larger discrepancies with the other propellants are given later. Since the predicted I_{sp} is 7 to 14% lower (depending on the case) than the I_{sp} for an isentropic expansion to an area ratio of 360, the viscous effects are not too large. The agreement between the predicted and measured performance values, nevertheless, is so close that it provides a good verification of the accuracy of the calculation method. In fact, the accuracy of the predicted I_{sp} values for some of these cases is within the scatter in the experimental I_{sp} data ($\pm 1\%$).

For each case the maximum-thrust point occurs upstream of the nozzle exit plane. The area ratio at which the computed thrust coefficient reaches its maximum value is shown in Table 3. Furthermore, for each case the computed pressure gradient becomes positive upstream of the nozzle exit plane. Since Rae's computer program cannot handle an adverse pressure gradient, the computer run terminates at this point. The area ratio and pressure ratio at the end of the run are listed in Table 3. The thrust coefficient at this point was used in the comparison with the experimental data; this procedure is equivalent to assuming that the flow separates at this point. Since the computed thrust coefficient is changing very slowly at this point and the computed pressure ratio is very small, this assumption is not expected to produce a significant error in the predicted performance.

Reference 6 presents a theoretical correlation of ideal frozen-flow I_{sp} versus propellant molecular weight MW at $T_0 = 3000$°R, with $I_{sp} \propto (T_0/MW)^{1/2}$.

The correlation indicates how I_{sp} can increase with dissociation of methane at high temperatures. Even at a low temperature, dissociation effects may be evidenced. Thus the 1800°R methane experimental I_{sp} is seen to be higher than the predicted-227 sec vs 206 sec (Table 3). The 227-sec I_{sp} data point was taken after thermal steady state conditions were established. For all practical purposes, instantaneous thrust was constant and a valid data point was obtained. However, over several hours at the 1800°R condition, thrust was found to decrease slowly at 0.1%/hr. This slow rate of thrust decrease was due to a very slow closing of the nozzle throat due to carbon deposition from which it was concluded that the methane was being reacted. The extent of the reaction was unknown, however. Reaction of a portion of the methane to hydrogen for example,

$$CH_4 \rightleftharpoons C^* + 2H_2 \tag{8}$$

would result in an increase in specific impulse and may account, in part at least, for the discrepancy between predicted and experimental I_{sp} for CH_4 at 1800°R.

It should be pointed out that, in comparing the experimental data (good to within 1%) with the predicted, a deduced chamber temperature is used which is not directly measured. Differences of as much as 3% in the experimental I_{sp} vs predicted are therefore to be expected. That is, even if both the experimental data and predicted performance were exact in themselves, an estimated 3% difference is possible in not being able to define a corresponding exact chamber temperature for the experimental case. In this respect, had enough points been compared, an indication of the validity of the predictions based on the experiments would lie in a statistical

Table 3 Predicted vs measured performance

Gas	T_0, °R	B	ϵ at Max C_F	Conditions at end of run		I_{sp}, sec		Percent difference
				ϵ	p/p_0	Predicted	Measured	
H_2	3,000	1,980	128	136	9.7×10^{-4}	630	630	0.0
H_2O	2,800	3,990	228	261	4.1×10^{-4}	234	235	−0.4
H_2	1,400	4,700	136	143	4.5×10^{-4}	431	436	−1.1
CH_4	1,800	5,480	296	346	3.6×10^{-4}	206	227	−9.2
CO_2	2,200	8,970	250	273	3.3×10^{-4}	150	143	+4.9
CH_4	1,200	10,120	296	333	2.9×10^{-4}	168	172	−2.3
H_2O	1,260	13,190	228	228	3.1×10^{-4}	166	161	+3.1

average of the differences having a value close to zero. With the exception of the 1800°R methane data shown above to be high in measured value on the basis of dissociation, the RMS deviation for the differences is found to be 2.6%. Too few data points are available to assign any significance to this value. A simple arithmetic mean which accounts for the sign of each data point difference is significant, however. The differences average to +0.7% (predicted higher than experimental) for the remaining cases.

Aside from the 1800°R CH_4 data, the remaining two relatively large differences occur with CO_2 and 1260°R H_2O. The only explanation which can be given for the CO_2 case is that chamber temperature deduction from an energy balance is least accurate for low power consumption CO_2 propellant. In the case of the water, however, with a nominal degree of superheat of 540°R, condensation conditions would be expected in the nozzle expansion and could explain why the experimental I_{sp} is lower than the predicted value.

The fact that the 3000°R hydrogen I_{sp}, predicted vs experimental, agrees exactly is not necessarily a coincidence. At 3000°R with H_2, power consumption of the thruster is higher than for the other propellants. In addition, hydrogen is the best heat transfer fluid of the propellants tested. In effect, the power losses on a percentage basis are considerably less for hydrogen than for the other propellants. In this situation, chamber temperature estimates from an energy balance evaluation are considerably more accurate with hydrogen than with any of the other propellants.

Another observation that can be made from the Table 3 values is with regard to the tendency of the measured I_{sp} to become less than predicted as Reynolds number B increases. Again, the 1800°R CH_4 is taken as an exception for the aforementioned reasons. This tendency would indicate that divergence losses are becoming important with increasing B and reduced subsonic boundary layer thickness. That is, the large ε, wide divergence angle trumpet nozzle works well at low B but not as well, relatively speaking, at the higher B. This trend is to be expected from theoretical considerations.

Finally, it is important to note that the chamber temperatures used in the Rae computations (Tables 2 and 3) were those derived from the experimental data and were not subsequently influenced by the performance predictions. The data presented in this paper reflect predicted specific impulses independent of measured values as derived from the chamber temperature estimates. In this respect, it is conceivable, once confidence is gained in the prediction method, to turn it around for chamber temperature predictions based on measured specific impulse. In view of the considerations mentioned, the predicted values appear sufficiently accurate to recommend use of the modified Rae method for space station design calculations.

Conclusions

The Rae computer program was modified and used to predict low thrust, thick boundary-layer flow in small nozzles using typical biowaste expendables from a Sabatier life support system as propellants. Data were obtained for flowfield in and performance of a 25-mlb thruster with a conical nozzle suitable for space station attitude control. A comparison of inviscid expansion with the Rae viscous flow program showed the latter to have lower values of I_{sp} (as much as 12%), higher pressure ratios, higher temperature ratios, and lower velocities, all of which would affect previously predicted thruster performance data as well as exhaust plume characteristics.

The Rae program was also run for high and low chamber temperature gases using a 10-mlb thruster with a trumpet nozzle, and the computed results were compared with experimental data. The experimental data were, in general, believed valid within 1%. However, the chamber temperature, which was an essential input to the Rae program, was not directly measured in the thruster but was instead derived by energy balance calculations involving methods which could result in a 3% error between measured and predicted performance. For the pure gases H_2, H_2O, and CO_2, the predicted I_{sp} values are, on the average, 0.7% higher than those of the experimental data indicating that the test trumpet nozzle used delivered performance within about 1% of optimum. In the case of CH_4, at 1800°R, a relatively large difference between predicted and test I_{sp} value is attributed to dissociation reactions.

From the comparison data, it appears that the Rae program is a useful and accurate tool for predicting low-thrust viscous nozzle performance with nonreactive gases. This program is, therefore, an essential adjunct for determining the performance of a single universal design using a variety of propellant compositions as would be the case for an actual mission.

References

[1] Bliss, J. R. and Greco, R. V., "Design and Operational Characteristics of an Integrated Biowaste Resistojet System," AIAA Paper 71-686, Salt Lake City, Utah, 1971.

[2] Gaubatz, W. A., James, N. E., and Page, R. J., "Chemical Nonequilibrium Effects in Biowaste Thruster Performance," AIAA Paper 71-688, Salt Lake City, Utah, 1971.

[3] Rae, W. J., "Final Report on a Study of Low-Density Nozzle Flows, with Application to Microthrust Rockets," Rept. AI-2590-A-1, Contract NASW-1668, Dec. 1969, Cornell Aeronautical Lab.; also *AIAA Journal*, Vol. 9, No. 5, May 1971, pp. 811–820.

[4] Halbach, C. R., "Ten-mlb Biowaste Resistojet Performance," AIAA Paper 71-687, Salt Lake City, Utah, 1971.

[5] Goodman, M. and Yakut, M. M., "Advance Biowaste Electric Propulsion Systems," *Transactions of the ASME: Journal of Engineering for Industry*, Vol. 92B, Aug. 1970, pp. 613–620.

[6] Halbach, C. R. and Yoshida, R. Y., "Development of a Biowaste Resistojet," *Journal of Spacecraft and Rockets*, Vol. 8, No. 3, March 1971, pp. 273–277.

[7] Rothe, D. E. "Electron-Beam Studies of Viscous Flow in Supersonic Nozzles," *AIAA Journal*, Vol. 9, No. 5, May 1971, pp. 804–811.